MRS Advances © 2017 Materials Research Society
DOI: 10.1557/adv.2017.384

Reaction kinetics of $Cu_{2-x}S$, ZnS, and SnS_2 to form Cu_2ZnSnS_4 and Cu_2SnS_3 studied using differential scanning calorimetry

Elizabeth A. Pogue, Melissa Goetter[1] and Angus Rockett[1,2]
[1]University of Illinois Urbana-Champaign, Department of Materials Science and Engineering, Champaign, IL 61801, U.S.A.
[2]Colorado School of Mines, Department of Metallurgical and Materials Engineering, Golden, CO 80401, U.S.A.

ABSTRACT

Differential scanning calorimetry experiments on mixed $Cu_{2-x}S$, ZnS, and SnS_2 precursors were conducted to better understand how Cu_2ZnSnS_4 (CZTS) and Cu_2SnS_3 form. The onset temperatures of Cu_2SnS_3 reactions and CZTS suggest that the ZnS phase may mediate Cu_2SnS_3 formation at lower temperatures before a final CZTS phase forms. We also found no evidence of a stable $Cu_2ZnSn_3S_8$ phase. The major diffraction peaks associated with Cu_2ZnSnS_4, and Cu_2SnS_3 (overlaps with ZnS, as well) began to grow around 380 °C, although the final reaction to form Cu_2ZnSnS_4 probably did not occur until higher temperatures were reached. An exothermic reaction was observed corresponding to formation of this phase. There was some variability in the onset temperature for reactions to form Cu_2SnS_3. At least 5 steps are involved in this reaction and several segments of the reaction had relatively reproducible energies.

INTRODUCTION

Cu_2ZnSnS_4 (CZTS) solar cell efficiency improvements have proven difficult since 2013 [1], suggesting that new approaches informed by the system's fundamental thermodynamics and common kinetic routes is needed. Cu_2SnS_3-based solar cells are also being investigated as another non-toxic, Earth-abundant absorber layer option, although efficiencies do not yet match those of CZTS-based cells. Consequently, understanding how either of these phases form might help explain some of this performance gap.

The energy landscape for the Cu-Zn-Sn-S system is not fully understood. Experimental data exist for the ZnS, SnS_2, CZTS, and Cu_2S phases (see Figure 1). A calculated Cu_2SnS_3 formation enthalpy has been reported [2]. The formation enthalpy of monoclinic Cu_2SnS_3 has been calculated, although no experimental results exist. Unfortunately, the calculated formation enthalpy for Cu_2SnS_3 is less negative than the experimental formation energy for its constituent binary sulfides, Cu_2S+SnS_2. This is likely due to a systemic calculation error. The magnitude of that error can be estimated to be -0.5 eV by comparing experimental and calculated formation energies of SnS_2 and Cu_2S. This suggests that the Cu_2SnS_3 phase has a higher (less negative) formation energy than CZTS. One would not expect CZTS to decompose into ZnS and Cu_2SnS_3 due to their formation energies.

Several groups have conducted high-temperature x-ray diffraction (HT-XRD) investigations to understand how CZTS forms with temperatures ranging from slightly below 300 °C to 570 °C. According to Schurr et al., $Cu_{2-x}S$ and SnS_2 react between 415 and 542 °C to produce Cu_2SnS_3. This then reacts with ZnS near 572 °C to form the final CZTS phase [3]. For Cu-poor compositions, Cu_4SnS_6 was observed as an intermediate phase that formed around 177 °C and melted around 537 °C before the final CZTS phase formed. CZTS formation

temperatures between 450 and 500 °C [4], of 350-430°C [5], and slightly less than 300 °C [6] have been reported by other authors. All agreed that CZTS likely formed through Cu_2SnS_3 reacting with ZnS. Some of this variability may be related to different temperature ramp rates or the precise sample stoichiometry. Our study controls for sample stoichiometry variability by employing well-characterized binary sulfide precursors and compares results from different techniques obtained using different ramp rates.

EXPERIMENT

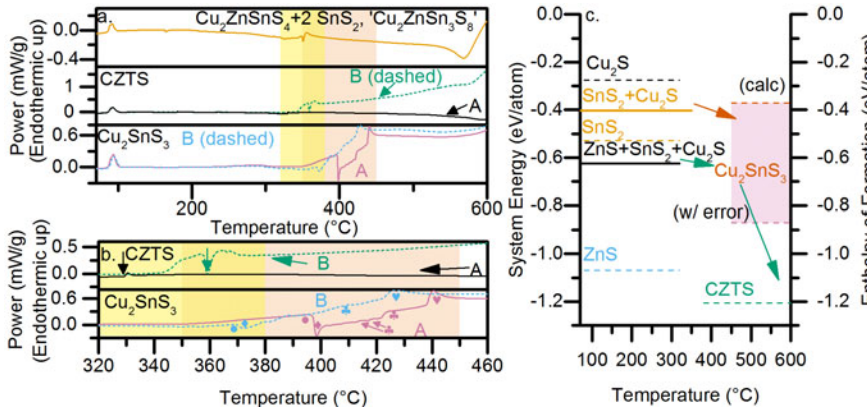

Figure 1. (a) shows the overall shape of DSC temperature ramps. (b) The highlighted regions in (a) where a series of at least 5 reactions can be distinguished for Cu_2SnS_3 and variability in the magnitude of CZTS energies is noted. (c) shows the formation energies of CZTS (experiment)[7], Cu_2SnS_3 (calculated)[2], and relevant binaries (experiment)[8] for context.

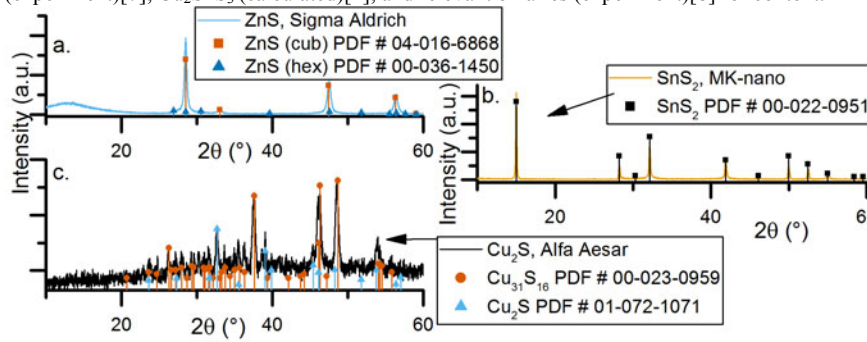

Figure 2. The ZnS precursor (a) was >95 % sphalerite (cubic) ZnS with a fraction of hexagonal ZnS too small to be determined using whole-pattern fitting. The SnS_2 precursor (b) was phase-pure hexagonal SnS_2. The Cu_2S precursor (c) matched well with a single low chalcocite (monoclinic) Cu_2S diffraction pattern (PDF # 04-007-1284) although, a slightly better match could be attained by invoking both Cu_2S (PDF # 01-072-1071) and $Cu_{31}S_{16}$ (PDF # 00-023-0959) references. Consequently, the Cu_2S should be slightly sulfur-rich.

Samples were synthesized by combining $Cu_{2-x}S$ (Alfa Aesar, 99.5 % -200 mesh), ZnS (Sigma Aldrich, 99.999%, 10 μm), and SnS_2 (MK Impex, +99 %, 3 μm) powders (characterized in Figure 1) in the appropriate stoichiometric ratios intended to form the pure Cu_2SnS_3, Cu_2ZnSnS_4, and $Cu_2ZnSn_3S_8$ phases. These were mixed in 350 mg batches in an Ar-filled glove box to ensure the absence of oxygen or water vapor, which could influence the results. X-ray diffraction patterns of the precursors were collected to verify their phase and composition, as shown in Figure 2. Each batch was divided into several aluminum differential scanning calorimetry (DSC) sample pans and one quartz capillary for HT-XRD measurements. Consequently, composition variations should only be attributable to the precise distribution of precursor powder grains in each sample, which should be minimal. The aluminum DSC sample pans, which were designed to be used with volatile samples (Perkin Elmer, part B0143016) were hermetically sealed by crimping. DSC scans were conducted using a Perkin Elmer DSC 7 power-compensated instrument calibrated for temperature and heat flow within 10 days of the reported measurements. The samples were weighed to the nearest 0.001 mg. To ensure accurate sample mass measurement, the weight of the empty pans was first measured and then the weight of the filled pans was measured.

A baseline DSC scan was conducted with empty sealed pans. Samples were heated to 600 °C at 20 °C/min. Samples were then held at 600 °C for 1 minute. They were then cooled at 20 °C/min to 50 °C, although this cooling rate was less well-controlled than the heating. The samples were reheated to 600 °C for a second time at 20 °C/min, held at 600 °C for 1 minute, and then cooled at 20 °C/min to 50 °C. One of the empty pans was replaced with a filled sample pan and another scan was performed using the same temperature profile. The baseline scan was subtracted from the sample scan. No reproducible features were observed in the second temperature ramp, demonstrating that these reactions were irreversible and no reversible phase transformations were found. The samples were weighed again. No mass changes greater than 0.09 mg were observed (<0.52 % of the initial sample mass), confirming that the hermetic seals did not leak significantly. The samples were then broken open for X-ray diffraction (XRD) and Raman analysis of the reacted material. Due to the small sample sizes (~16 mg), it was necessary to spread the samples on pieces of tape mounted on glass slides for analysis. XRD measurements were collected using a Panalytical/Philips X'Pert 2 MRD system, using Cu k-α radiation. To confirm that there were no reactions occurring with the Al pan, ω-2θ scans were also collected on the interior bottom of at least one pan per sample type. No such reactions were observed. Samples were then investigated using a Horiba LabRAM HR 3D Raman Confocal Imaging Microscope with a 1800 gratings/mm grating at 50 x magnification. No significant intra-sample variation was observed (at least 3 measurements/sample). In-situ high-temperature x-ray diffraction measurements were conducted using a Bruker D-8 diffractometer with Mo k-α radiation from room-temperature to 600 °C on the powder mixture with the CZTS composition at a 1 °C/min heating rate. Higher temperatures caused the capillary to break.

RESULTS AND DISCUSSION

The DSC data are presented in Figure 1. As the precise distribution of binary precursors in the Cu_2SnS_3 and CZTS samples changed, the reaction onset temperatures shifted. In the CZTS sample, the magnitude of some transitions also changed. For example, transitions of significantly different magnitudes and temperatures were observed between 325 and 380 °C, even though both

samples came from the same mixture batch. Furthermore, the $Cu_{2-x}S$ content was confirmed to be equal since there is no difference in the endothermic DSC peak at 100 °C. The height of this peak is also proportional to the phase fraction of $Cu_{2-x}S$ in the "$Cu_2ZnSn_3S_8$" sample. This sample produced SnS_2 and CZTS by the end of the scan. The endotherm observed near 100 °C corresponds to a transition between the monoclinic γ-Cu_2S/$Cu_{31}S_{16}$ and hexagonal β-Cu_2S phases [9]. No difference was observed between the post-reaction diffraction patterns of CZTS samples A and B (only CZTS was observed). However, the Raman measurements, shown in Figure 3, showed broader peaks in sample B and the main Raman mode was shifted to lower wavenumbers, 332 cm^{-1} in B vs. 338 cm^{-1} in A. This suggests that the CZTS in A had different and likely improved ordering compared to B. Valakh *et al.* observed, within a single sample, a wholesale shift in Raman peaks to lower wavenumbers in more lightly colored portions of the film and attributed this shift to more Cu-Zn disorder regions exhibiting a 332 cm^{-1} peak compared to regions with a peak at 338 cm^{-1}[10]. Dimitrievska *et al.* suggested that phonon confinement may result in a 332 cm^{-1} peak, although this would not explain the laser power dependence of the peak shift they observed [11]. Paris *et al.* similarly cast doubt on Valakh *et al.*'s explanation by observing that samples quenched from 750 °C did not show a significant peak shift compared to slow-cooled samples [12]. They synthesized both stoichiometric and off-stoichiometric samples targeting Cu-Zn disorder and did not see any peak shift, making it unlikely that compositions Cu-Zn disorder is responsible [12]. Our results suggest that the 332 cm^{-1} peak may be related to the precise the synthesis route. We found no evidence of a $Cu_2ZnSn_3S_8$ phase in any sample by any method.

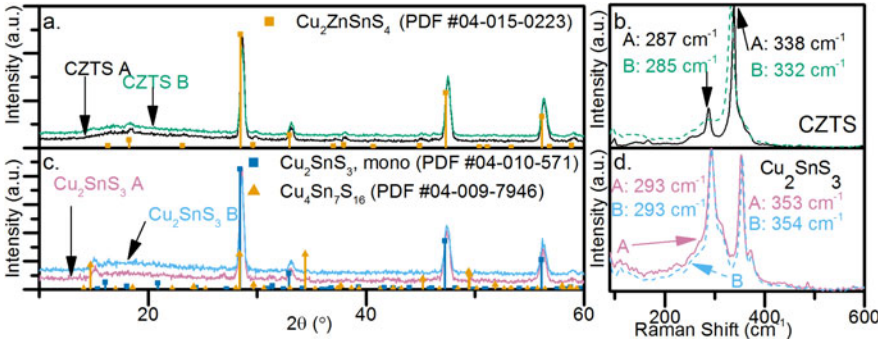

Figure 3. XRD (a. and c.) and Raman (b. and d.) results shown that kesterite CZTS (a. and b.) and monoclinic Cu_2SnS_3 (c. and d.) are the final products of the DSC scans as expected by the initial mixtures. The CZTS samples did not contain any detectable secondary phases. The Cu_2SnS_3 samples contained small amounts of $Cu_4Sn_7S_{16}$ secondary phase but was mostly monoclinic Cu_2SnS_3.

The route to form Cu_2SnS_3 showed less variability than that of CZTS, producing a more consistent final product (Figure 3) after undergoing at least 5 reactions. The energies of these reactions are extracted from the DSC data and presented in Table I. The final products consisted of primarily monoclinic Cu_2SnS_3 with some disordered regions more like cubic Cu_2SnS_3 (as evidenced by a ~300 cm^{-1} shoulder to the 293 cm^{-1} mode).

Table I. A summary of measured transition energies. Peaks 2 and 5 are reproducible and peaks 3 and 4 summed together for each sample are approximately equal.

		Cu_2SnS_3			
		A		B	
#		Onset T (°C)	Energy (J/g)	Onset T (°C)	Energy (J/g)
1	●	371± 3 °C	14 ± 4 J/g	358.8 ± 0.6 °C	0.8 ± 0.3 J/g
2	♦	398.0 ± 0.3 °C	-1.47 ± 0.09 J/g	370.4 ± 0.3 °C	-1.3 ± 0.3 J/g
3	♣	413.3 ± 1.1 °C	0.17 ± 0.04 J/g	385.0 ± 1.8 °C	0.74 ± 0.02 J/g
4	♣	421.72 ± 0.03°C	1.9 ± 0.3 J/g	402.4 ± 0.6 °C	0.60 ±0.08 J/g
5	♥	438.5 ± 1.1°C	6.0 ± 1.4 J/g	422.85 ± 0.10°C	4.9 ± 0.8 J/g

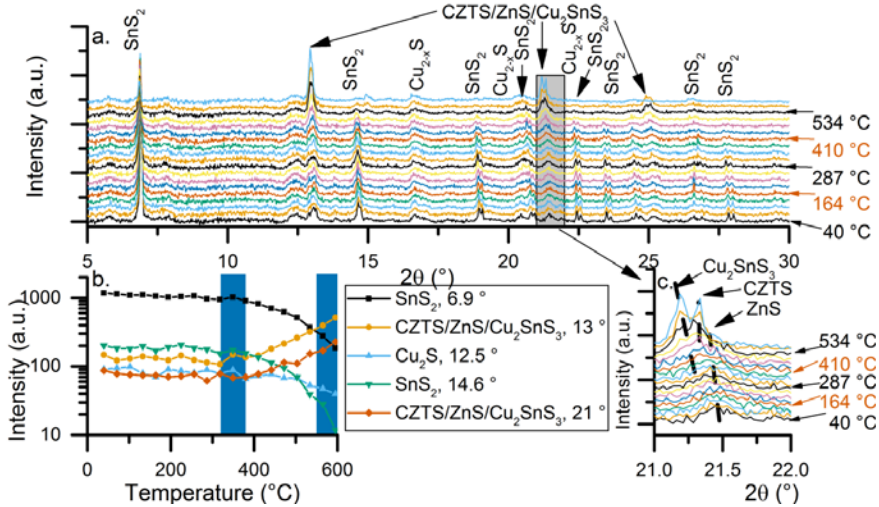

Figure 4. HT-XRD (Mo k-α) demonstrates that Cu_2S and SnS_2 begin to react between 320 and 380 °C. The full scan is shown in (a.) with a zoomed-in section in (c.). The intensity of selected peaks is monitored in (b.). These intensities were determined by selecting a window around the peak and finding the maximum value within that window.

The HT-XRD results (Figure 4) show that Cu_2SnS_3 begins to form from Cu_2S and SnS_2, based on changes in the corresponding peaks, between 320 and 380 °C in agreement with the DSC results. The formation temperature of $Cu_2SnS_3$was identified by noting the temperature at which Cu_2S and SnS_2 peaks decrease in intensity and Cu_2SnS_3 peaks begin to rise. The reaction to form CZTS is difficult to distinguish from Cu_2SnS_3 based on the overlap of the peak positions and low intensity intensity of unique peaks. However, at elevated temperatures, the main (but overlapping) CZTS, Cu_2SnS_3, and ZnS peaks begin to diverge due to thermal expansion. For scans at ≥560 °C there is a noticeable decrease in the high-angle side of the peak associated with ZnS. The lower angle side of the peak correlates best with Cu_2SnS_3. At ~473°C a central component, probably due to CZTS was observed and the peak narrowed, suggesting

disappearance of the reactants. We conclude that the high-temperature exothermic transition observed using the DSC between 550 and 600 °C was associated with Cu_2SnS_3 and ZnS reacting to form CZTS. The difference between the temperature observed in the XRD and in the DSC was the result of the difference in heating rate (1 °C/min for HT-XRD and 20 °C/min for DSC).

CONCLUSIONS

The reactions of Cu_2S and SnS_2 to form Cu_2SnS_3 were found to include at least 5 steps. ZnS seems to mediate the reaction, lowering the reaction temperature in samples where it is present. High-temperature x-ray diffraction shows that the ZnS/Cu_2SnS_3/CZTS peak begins to increase around 380 °C due to the formation of Cu_2SnS_3 and above 540°C due to Cu_2ZnSnS_4. Reaction energies for Cu_2SnS_3 were extracted from the DSC data. The reaction of Cu_2SnS_3 and ZnS to form CZTS is exothermic.

ACKNOWLEDGMENTS

This project was funded by the National Science Foundation (NSF) SEP Collaboration Contract NSF CHE 12-30973. Experiments were conducted at the Frederick Seitz Materials Research Laboratory Central Facilities and the Beckman Institute. The Shoemaker research group facilities were used for HT-XRD experiments and packing precursor powders in DSC sample pans.

REFERENCES

1. W. Wang, M.T. Winkler, O. Gunawan, T. Gokmen, T.K. Todorov, Y. Zhu, and D.B. Mitzi, Adv. Energy Mater. **4**, 1301465 (2014).
2. T. Maeda, S. Nakamura, and T. Wada, Jpn. J. Appl. Phys. **50**, 04DP07 (2011).
3. R. Schurr, A. Hölzing, S. Jost, R. Hock, T. Voβ, J. Schulze, A. Kirbs, A. Ennaoui, M. Lux-Steiner, A. Weber, I. Kötschau, and H.-W. Schock, Thin Solid Films **517**, 2465 (2009).
4. A. Fairbrother, X. Fontané, V. Izquierdo-Roca, M. Espíndola-Rodríguez, S. López-Marino, M. Placidi, L. Calvo-Barrio, A. Pérez-Rodríguez, and E. Saucedo, Sol. Energy Mater. Sol. Cells **112**, 97 (2013).
5. A. Weber, R. Mainz, T. Unold, S. Schorr, and H.-W. Schock, Phys. Status Solidi **6**, 1245 (2009).
6. S. Schorr, A. Weber, V. Honkimäki, and H.W. Schock, Thin Solid Films **517**, 2461 (2009).
7. S. V. Baryshev and E. Thimsen, Chem. Mater. **27**, 2294 (2015).
8. O. Kubaschewski, C.B. Alcock, and P.J. Spencer, *Materials Thermochemistry*, 6th ed. (Pergamon Press, New York, 1993) pp. 258-323.
9. M.J. Buerger and B.J. Wuensch, Science (80-.). **141**, 276 (1963).
10. M.Y. Valakh, V.M. Dzhagan, I.S. Babichuk, X. Fontane, A. Perez-Rodriquez, and S. Schorr, JETP Lett. **98**, 255 (2013).
11. M. Dimitrievska, A. Fairbrother, A. Pérez-Rodríguez, E. Saucedo, and V. Izquierdo-Roca, Acta Mater. **70**, 272 (2014).
12. M. Paris, L. Choubrac, A. Lafond, C. Guillot-Deudon, and S. Jobic, Inorg. Chem. **53**, 8646 (2014).